EXPERIMRNTAL VALIDATED CFD ANALYSIS ON HELIUM DISCHAR

J.C. Chang,* Y.C. Chang, F.Z. Hsiao, S.P. Kao, H.C. Li, W.R. Liao, C.Y. Liu
National Synchrotron Radiation Research Center, Hsinchu 30076, Taiwan
* jcchang@nsrrc.org.tw

MEDSI 2016
MECHANICAL ENGINEERING DESIGN OF SYNCHROTRON RADIATION EQUIPMENT AND INSTRUMENTATION
TUPE02

Abstract

National Synchrotron Radiation Research Center in Taiwan (NSRRC) had set up three cryogenic systems to provide liquid helium to superconducting radio-frequency (SRF) cavities, insertion devices, and highly brilliant hard X-ray. The first one could produce liquid helium 134 LPH, with maximum cooling capacity of 469 W at 4.5 K. The second one could produce liquid helium 138 LPH, with maximum cooling capacity of 475 W at 4.5 K. The third one could produce liquid helium 239 LPH, with maximum cooling capacity of 890 W at 4.5 K. However, large liquid helium discharge in a closed space will cause personnel danger of lack of oxygen. We performed Computational Fluid Dynamic (CFD) simulation to analyse helium discharge through a SRF cavity in the Taiwan Light Source (TPS) tunnel. We simulated cases of helium discharge flow rates from 0.1 kg/s to 4.2 kg/s with and without fresh air supplied from the air conditioning system. We also set up both physical and numerical models within a space of 2.4m in length, 1.2m in width and 0.8m in height with nitrogen discharge inside to validate the CFD simulation.

INTRODUCTION

Liquid helium for transferring cooling power from the cryogenic plant to the magnets and SRF cavities had been widely applied on the advanced large superconducting particle accelerators. For requirements of high stable and reliable operation, many efforts have been put into the improvement and modification of the cryogenic system.

One cryogen distribution system has been installed and commissioned to transfer liquid nitrogen and LHe from storage dewars to superconducting radio-frequency (SRF) cavities at TPS. The cryogenic system has maximum cooling capacity 890 W with associated compressors, an oil-removal system, four helium buffer tanks, one 7000-L Dewar, gaseous helium piping at room temperature, transfer lines to distribute helium, and a transfer system for liquid nitrogen. Currently, there are two SRF cavities are located one upstream and one downstream of the distribution valve box.

Personnel safety is another critical issue of the cryogenic system. Once large liquid helium (LHe) was released on the atmospheric tunnel, the volume of helium will expand several hundred times in short time due to sudden change of its density. Therefore, cold helium discharge test in the LHC tunnel at CERN had been experimentally conducted. Numerical simulation of cold helium safety discharges had also been performed at European Spallation Source (ESS).

NUMERICAL SIMULATION

Detailed 3D numerical simulation was performed using a commercial general purpose CFD code ANASYS Fluent. We apply the k-ε turbulence model and SIMPLEC to solve the velocity and pressure problem.

Governing equation

Mass conservation equation

$$\frac{\partial \rho}{\partial t} + \nabla \cdot (\rho \mathbf{u}) = 0$$

where ρ is density of fluid, t is time and u refers to fluid velocity vector.

Momentum conservation equation

$$\frac{\partial (\rho \mathbf{u})}{\partial t} + \nabla \cdot (\rho \mathbf{u}\mathbf{u}) = -\nabla p + \rho \mathbf{g} + \nabla \cdot (\mu \nabla \mathbf{u}) - \nabla \cdot \tau_t$$

where p is pressure, g is vector of gravitational acceleration, μ is dynamic viscosity of fluid.

Energy conservation equation

$$\frac{\partial (\rho e)}{\partial t} + \nabla \cdot ((\rho e + p)\mathbf{u}) = \nabla \cdot \left(k \nabla T - \sum_j h_j \mathbf{j}_j \right)$$

where e is the specific internal energy, T is fluid temperature, k is heat conductivity, h is the specific enthalpy of fluid.

Boundary Conditions

The flowrate of helium discharge was given the worst case of 4.2 kg/s by our SRF people. Time of helium discharge is 10 s. There are two simulation cases A and B in this study. Case A: Discharge helium flows vertically upward. Case B: Discharge helium flowing toward the exhaust blower on inner wall. Other initial and boundary conditions are list as follow.

1. Air temperature in the tunnel is 25 ˚C at t = 0s.
2. Discharged helium temperature is 4 K.
3. Wall and floor are adiabatic.
4. Both sides are opened to atmosphere (1atm).
5. Supplied air flow velocity is 2 m/s from air exits.
6. Back pressure of the air exhaust is 1000pa.

Geometry and Grid Generation

A detailed 3D model of 2 of 24 sections of the TPS tunnel, where a SRF cavity is located, was built for the numerical simulation. The space of the simulation zone is about 860.5 m^3. The geometry was built according to the dimensions of the tunnel, as shown in Fig.1. The total number of the grid elements was about 3.34 million. The size of relevance center was fine. The minimum grid element size is 0.00177m near the helium discharge exit.

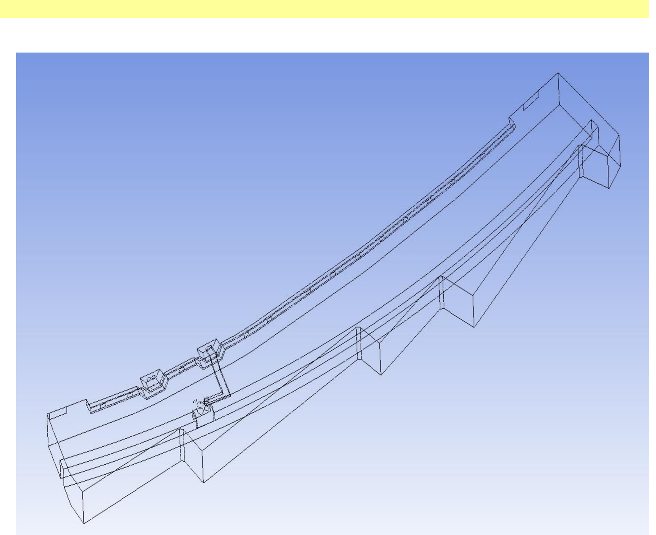

Figure 1: Numerical model.

RESULTS AND DISCUSSION

We select a monitor plane at the z= 1.5 m, about at the height of one's nose. Fig. 2 shows the simulation results of helium mass fraction of cases A and B on the plane z =1.5 m at t = 10s. The simulated helium mass fraction is distributed from 6.567% to 0.2%. It can be observed that the helium mass fraction of case B is lower than that of case A due to the effect of the exhaust blower. High helium mass fraction is shown on the wedge area near the outer wall in case A because that a circulation forms in that area. On the other hand, the helium mass fraction is higher in the area between the helium discharge exit and the exhaust blower in case B.

Fig. 3 shows the simulation results of helium mass fraction of cases A and B on the plane z =1.5 m at t = 30s. The helium mass fractions of both cases at t = 30s are clearly lower than that at t =10s. However, some residual helium still remains on the wedge area near the outer wall in case A and in the area between the helium discharge exit and the exhaust blower in case B. On the hand, the helium mass fraction is higher in the area between the helium discharge exit and the exhaust blower in case B.

We also simulate the case without fresh air supplied by the air conditioning system. Fig. 5 shows the simulation results of helium mass fraction of cases without supplied air on the plane z =1.5 m at t = 10s (A) and t = 30s (B). Higher helium mass fraction simulation results are shown in Fig. 4 (A) and (B) than the cases with supplied air shown in Figs. 2 and 3.

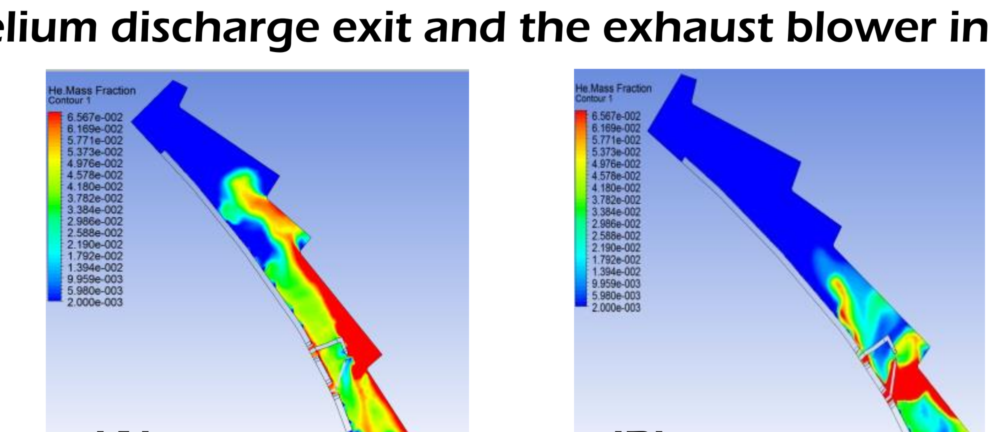

(A) (B)

Figure2: Simulation results of helium mass fraction of cases A and B on the plane z =1.5 m at t = 10s.

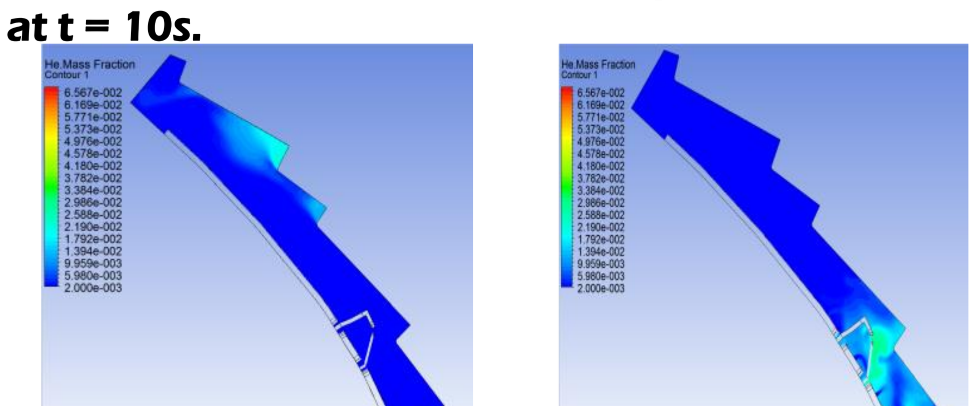

(A) (B)

Figure3: Simulation results of helium mass fraction of cases A and B on the plane z =1.5 m at t = 30s.

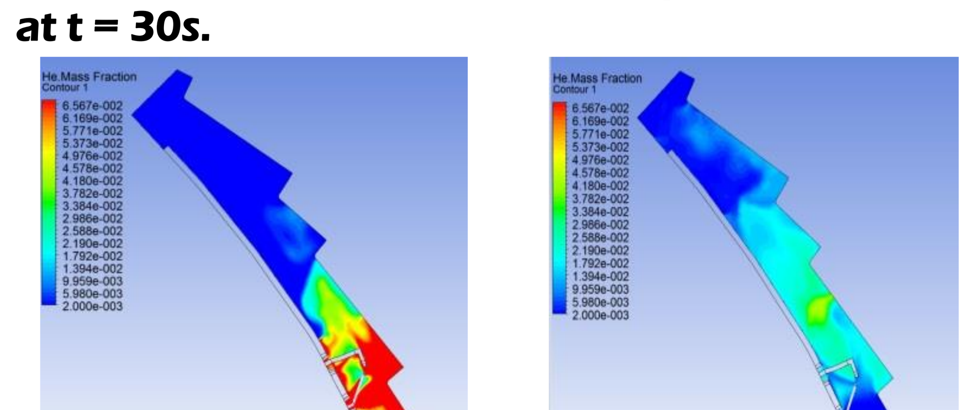

(A) (B)

Figure4: Simulation results of helium mass fraction without supplied air on the plane z =1.5 m at t = 10s (A) and 30s.(B)

EXPERIMENTAL VALIDATION

A cubical space of 2.4m in length, 1.2m in width and 0.8m in height with nitrogen discharge inside. The cubical cover was made of transparent acrylic. Another small cubic box of 1.2m in length, 0.2m in width and 0.4m in height was installed inside. The nitrogen discharge exit is located on the top of the small cubic box. An air exhaust hole was located on the upper area of the wall, as shown in Fig. 5, the geometry of the experiment.

Two oxygen sensors were put on the small cubic box. The range and resolution of the sensor are 0-30% and 0.1%, respectively. Three T-type thermocouples are installed at the nitrogen inlet, air exhaust and on the box. A flowrate multi-meter is installed at the nitrogen inlet. Fig. 6 shows the experiment with nitrogen discharge in the cubic space. We also set up a 3D numerical model to simulate the experiment case. The total number of the grid elements was about 180,000. Fig. 7 shows the simulation results of O2 mass fraction. Low O_2 mass fraction is shown near the nitrogen exit. The profile of low O_2 mass fraction is similar to that of experimental result shown in Fig. 6.

Fig. 8 shows experimental and simulation results of oxygen concentration. Although the experimental data is lower than the simulated ones, slopes of curves are close.

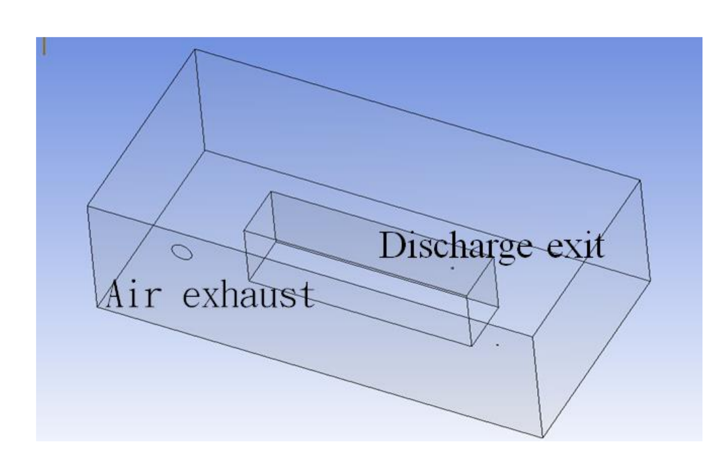

Figure5: Geometry of the experiment.

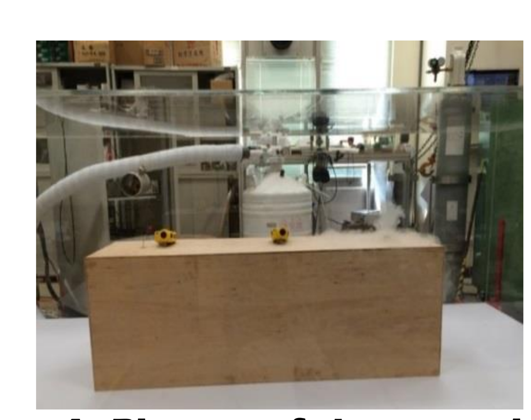

Figure 6: Picture of the experiment.

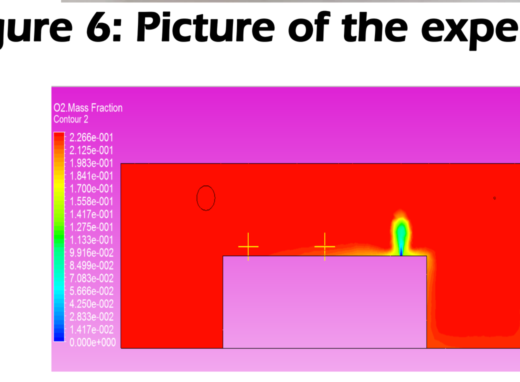

Figure 7: Simulation results of O_2 mass fraction.

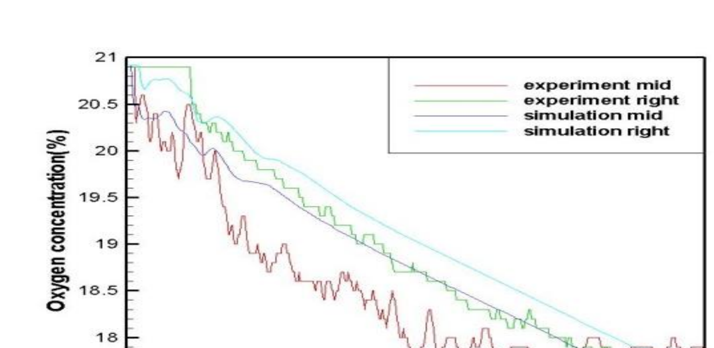

Figure 8: Experimental and simulation results of oxygen concentration.